Gravitational waves from metastable cosmic strings in the Pati-Salam model in light of new pulsar timing array data

Waqas Ahmed,[1,†] Talal Ahmed Chowdhury,[2,3,4,‡] Salah Nasri,[5,4,*] and Shaikh Saad[6,§]

[1]*Center for Fundamental Physics and School of Mathematics and Physics, Hubei Polytechnic University, Huangshi 435003, China*

[2]*Department of Physics, University of Dhaka, P.O. Box 1000, Dhaka, Bangladesh*

[3]*Department of Physics and Astronomy, University of Kansas, Lawrence, Kansas 66045, USA*

[4]*The Abdus Salam International Centre for Theoretical Physics, Strada Costiera 11, I-34014, Trieste, Italy*

[5]*Department of Physics, UAE University, P.O. Box 17551, Al-Ain, United Arab Emirates*

[6]*Department of Physics, University of Basel, Klingelbergstrasse 82, CH-4056 Basel, Switzerland*

(Received 31 August 2023; accepted 15 December 2023; published 9 January 2024)

A series of pulsar timing arrays (PTAs) recently observed gravitational waves at the nanohertz frequencies. Motivated by this remarkable result, we present a novel class of Pati-Salam models that give rise to a network of metastable cosmic strings, offering a plausible explanation for the observed PTA data. Additionally, we introduce a hybrid inflationary scenario to eliminate magnetic monopoles that arise during the subsequent phase transitions from the Pati-Salam symmetry to the Standard Model gauge group. The resulting scalar spectral index is compatible with Planck data, and the tensor-to-scalar ratio is anticipated to be extremely small. Moreover, we incorporate a nonthermal leptogenesis to generate the required baryon asymmetry in our framework. Finally, the gravitational wave spectra generated by the metastable cosmic strings not only correspond to signals observed in recent PTAs, including NANOGrav, but are also within the exploration capacity of both present and future ground- and space-based experiments.

DOI: 10.1103/PhysRevD.109.015008

I. INTRODUCTION

Gravitational waves (GWs) provide a unique window to probe fundamental physics. Recently, the International Pulsar Timing Array Collaboration presented convincing evidence of such isotropic stochastic GWs with frequencies in the nanohertz range [1–4]. Although this stochastic GW background can be formed from the culmination of GWs produced from the inspiraling and merging of the supermassive black holes in the Universe [5], there is room for a new physics explanation of such signal. Indeed, as pointed out in [6,7], the GWs produced from metastable cosmic strings are compatible [8–14] with the recent results (for works on GWs, in light of previous pulsar timing array (PTA) data, arising from cosmic strings, cf. Refs. [15–29]). Cosmic strings can form in the early Universe during the intermediate step(s) in the spontaneous symmetry breaking of a unifying gauge group to the Standard Model (SM) [30]. In this work, we investigate the possible production of metastable cosmic strings during the spontaneous symmetry breaking of the Pati-Salam gauge group [31,32], $SU(4)_C \times SU(2)_L \times SU(2)_R$ to the SM. The Pati-Salam model introduced the attractive idea of the quark-lepton unification and also incorporated the left-right symmetry [33–35]. Additionally, the model, automatically containing the right-handed neutrinos, can explain the smallness of the neutrino mass via the seesaw mechanism [36–40] and encompass the leptogenesis mechanism [41] to account for the matter-antimatter asymmetry of the Universe. Additionally, the model naturally allows for neutron-antineutron oscillation [42].

Particularly, we consider the supersymmetric (SUSY) Pati-Salam model [43–46] where we show that three viable symmetry-breaking scenarios can lead to metastable cosmic string networks capable of explaining the PTA results. Among these three possibilities, we focus on a particular model where the Pati-Salam symmetry is first broken to the left-right symmetry, $SU(3)_C \times SU(2)_L \times SU(2)_R \times U(1)_{B-L}$. In the next phase transition, breaking of $SU(2)_R \to U(1)_R$ generates superheavy monopoles. In the subsequent breaking, i.e., when the last intermediate symmetry breaks down to that of the SM gauge group, the phase transition

*Corresponding author: snasri@uaeu.ac.ae, salah.nasri@cern.ch
†waqasmit@hbpu.edu.cn, waqas.ahmed@nanograv.org
‡talal@du.ac.bd
§shaikh.saad@unibas.ch

associated with $U(1)_R \times U(1)_{B-L} \to U(1)_Y$ leads to cosmic string formation. Within this setup, we implement supersymmetric hybrid inflation at the last intermediate symmetry-breaking scale, hence efficiently inflating away monopoles but not the cosmic strings. If these last two symmetry-breaking scales almost overlap, metastable cosmic string networks are formed through the Schwinger nucleation. We find that the inflationary scenario incorporates the scalar spectral index consistent with Planck data, and the tensor-to-scalar ratio remains tiny. Interestingly, the new PTA data suggest that both the monopole and string formation scales must be close to 10^{15} GeV, which perfectly coincides with the seesaw scale, as well as providing the inflation scale and leading to successful nonthermal leptogenesis. Several gravitational wave observatories will fully test the stochastic gravitational wave background generated by the metastable string network.

The article is structured as follows. In Sec. II, we discuss the recent PTA data and the production mechanism of metastable cosmic string networks. In Sec. III, we introduce a class of Pati-Salam models leading to the formation of metastable cosmic string networks, and in Sec. IV, we fully construct one of the viable candidate models. In Sec. V, we provide the details of the SUSY hybrid inflation and give a detailed account of nonthermal leptogenesis arising in our scenario. Finally, we present the results in Sec. VI and conclude in Sec. VII.

II. METASTABLE COSMIC STRINGS AND PTA DATA

Cosmic strings are one-dimensional topological defects that arise when an Abelian symmetry is spontaneously broken. In this context, we use the Nambu-Goto string approximation, which assumes that the primary mode of radiation emission is in the form of GWs [47].

The macroscopic properties of these cosmic strings are defined by their energy per unit length, denoted as $\mu_{\rm cs}$, and referred to as the string tension. In our study, we explore models where the breaking of the Abelian symmetry is linked to the vacuum expectation value (VEV) of the multiplets that also give rise to masses to the right-handed neutrinos (RHNs). Consequently, the tension of the cosmic strings is determined by the corresponding symmetry-breaking scale,

$$\mu_{\rm cs} \sim 2\pi M^2, \tag{1}$$

where the order one coefficient is not shown explicitly (for details, see Ref. [48]). In the above equation, M refers to the symmetry-breaking scale (more specifically, the VEV of the scalar field that breaks the symmetry) that creates the cosmic string network.

On the contrary, when a simple group is broken down into a subgroup that includes an Abelian factor, it gives rise to the creation of monopoles [49,50]. However, to avoid the problem of overclosing the Universe, inflationary processes must eliminate these monopoles. Subsequently, in a later stage, after the remaining Abelian symmetry is broken, cosmic strings emerge. When the scales of monopoles and cosmic strings are in close proximity, Schwinger nucleation occurs, leading to the creation of monopole-antimonopole pairs [51–53] on the string, causing it to decay. In such a scenario, at the high frequency regime, the string behaves like a stable one, whereas at the lower frequency regime, its behavior deviates form stable strings. When these metastable strings decay depends on the ratio of the monopole and string formation scales,

$$\alpha = \frac{m_{\rm MP}^2}{\mu_{\rm cs}} \sim \frac{8\pi}{g^2}\left(\frac{M'}{M}\right)^2, \tag{2}$$

where M' represents the monopole creation scale, i.e., the symmetry-breaking scale (more specifically, the VEV of the scalar field that breaks the symmetry) that is responsible for the formation of monopoles, and $m_{\rm MP} \sim 4\pi M'/g$ denotes the mass of the monopole. Moreover, g stands for the relevant gauge coupling constant.

Cosmic strings lose their energy by gravitational radiation. For the case of stable strings, they keep emitting gravitational waves until all their energy is transferred to GWs, and the string network disappears. Although at early times, metastable strings behave like stable strings, at late times the network disappears due to monopole-antimonopole pairs eating the strings, as aforementioned. More specifically, this decay time is defined as

$$t_s = \Gamma_d^{-1/2}, \qquad \Gamma_d = \frac{\mu}{2\pi} e^{-\pi\alpha}. \tag{3}$$

As can be seen from the above equation, due to the strong exponential suppression, the metastable cosmic string network resembles a stable network for $\alpha^{1/2} \gg 10$.

Excitingly, the newly released PTA data [6] can be explained by GWs originating from metastable cosmic string networks. The data show a preference for string tension values in the range of $G\mu_{\rm cs} \sim 10^{-8}$–$10^{-5}$ (where the Newton's gravitational constant $G = 6.7 \times 10^{-39}$ GeV^{-2}; hence, $G\mu_{\rm cs}$ is a dimensionless quantity) for $\sqrt{\alpha} \sim 7.7$–8.3, with strong correlations between these two quantities [6]. Importantly, these results are in full agreement with constraints obtained from cosmic microwave background observations. Conversely, stable cosmic strings are not favored by the recent PTA results.

From the data, it is obtained that the 68% credible region in the $G\mu_{\rm cs} - \sqrt{\alpha}$ parameter plane overlaps with the third advanced LIGO-Virgo-KAGRA (LVK) bound [6]. However, most of the 95% credible region in the same parameter plane remains fully consistent with the data, favoring $G\mu_{\rm cs} \lesssim 10^{-7}$ and $\sqrt{\alpha} \sim 8$ [6] [for example, from Eq. (2), with $g = 0.7$, a ratio $M'/M = 1.117$ of the two

scales corresponds to $\sqrt{\alpha} \sim 8$). An interesting point to note is that $G\mu_{\rm cs} \sim 10^{-7}$ approximately corresponds to $M \sim 10^{15}$ GeV, which aligns perfectly with the type-I seesaw contribution to neutrino mass and also matches the correct scale for inflation.

III. METASTABLE COSMIC STRINGS FROM PATI-SALAM MODELS

First, we point out that within the Pati-Salam model, only three symmetry-breaking chains can give rise to a metastable cosmic string network. To demonstrate this, we first denote the various gauge groups as follows:

$$\begin{aligned}
G_{422} &\equiv SU(4)_C \times SU(2)_L \times SU(2)_R,\\
G_{421} &\equiv SU(4)_C \times SU(2)_L \times U(1)_R,\\
G_{3221} &\equiv SU(3)_C \times SU(2)_L \times SU(2)_R \times U(1)_{B-L},\\
G_{3211} &\equiv SU(3)_C \times SU(2)_L \times U(1)_R \times U(1)_{B-L},\\
G_{\rm SM} &\equiv SU(3)_C \times SU(2)_L \times U(1)_Y,\\
G_{31} &\equiv SU(3)_C \times U(1)_{\rm em}.
\end{aligned}$$

The breaking chains compatible with providing metastable cosmic strings are, therefore,

$$\text{Chain I: } G_{422} \xrightarrow[\langle\Phi_1\rangle]{m_{\rm red}} G_{3221} \xrightarrow[\langle\Phi_2\rangle]{m_{\rm blue}} G_{3211} \xrightarrow[\langle\Phi_{4,5}\rangle]{\rm cs} G_{\rm SM}. \quad (4)$$

$$\text{Chain II: } G_{422} \xrightarrow[\langle\Phi_2\rangle]{m_{\rm blue}} G_{421} \xrightarrow[\langle\Phi_1\rangle]{m_{\rm red}} G_{3211} \xrightarrow[\langle\Phi_{4,5}\rangle]{\rm cs} G_{\rm SM}. \quad (5)$$

$$\text{Chain III: } G_{422} \xrightarrow[\langle\Phi_{1,2}\rangle/\langle\Phi_3\rangle]{m_{\rm red},m_{\rm blue}} G_{3211} \xrightarrow[\langle\Phi_{4,5}\rangle]{\rm cs} G_{\rm SM}. \quad (6)$$

For each of these cases, the additional symmetry-breaking stage, namely, $G_{\rm SM} \to G_{31}$ is not shown explicitly. The representations (under the Pati-Salam group) of these fields playing a role in symmetry breaking are $\Phi_1 = (15,1,1)$, $\Phi_2 = (1,1,3)$, $\Phi_3 = (15,1,3)$, and $\Phi_4 = (4,1,2)$ [$\Phi_5 = (\bar{4},1,\bar{2})$]. Note that $G_{422} \to G_{3211}$ can be obtained via the VEVs of two fields $\Phi_1(15,1,1) + \Phi_2(1,1,3)$ or by the VEV of a single field $\Phi_3(15,1,3)$.

The topological defects arising in these breaking chains are denoted by $m_{\rm red}$ (red monopole), $m_{\rm blue}$ (blue monopole), and cs (cosmic string). The breaking of the gauge group $SU(4)_C \to SU(3)_C \times U(1)_{B-L}$ [$SU(2)_R \to U(1)_R$] leads to monopoles that carry both color and $B-L$ (only R) magnetic charges (charge) [which is referred to as the red (blue) monopole in Ref. [54]]. Finally, the last symmetry-breaking scale before the electroweak breaking, i.e., $U(1)_R \times U(1)_{B-L} \to U(1)_Y$ leads to the formation of cosmic strings. Following the discussion above, through the quantum tunneling of the monopole-antimonopole pairs, strings eventually disappear if the monopole and cosmic string formation scales almost coincide. Our primary focus of this work is on these metastable cosmic string networks that may have formed in the very early Universe, which emit gravitational waves that may have been observed in the PTAs.

Since inflation must eliminate the unwanted monopoles, within the supersymmetric framework, there are different possibilities for achieving this successfully. The simplest scenario is the standard hybrid inflation. Since, in this case, the waterfall happens at the end of the inflation, the only consistent option is that inflation takes place at the $G_{3211} \to G_{\rm SM}$ breaking stage. Consequently, the waterfall leading to cosmic string formation is not inflated away, however, monopoles are. Another possibility could be implementing shifted hybrid inflation [45,55], where inflation can occur at an earlier stage. For example, shifted hybrid inflation in which symmetry breaking $G_{421} \to G_{3211}$ proceeds along an inflationary trajectory can inflate away heavy monopoles (in principle, the same mechanism can be applied for the $G_{3221} \to G_{3211}$ or $G_{422} \to G_{3211}$ scenario).

IV. MODEL

Although each of the scenarios discussed in the previous section is worth exploring, we focus on a concrete model in this work, as detailed in the following. As mentioned in the Introduction, we work in the supersymmetric framework.

In the Pati-Salam model with gauge symmetry G_{422}, the SM fermions belong to the following representation:

$$F_i = (4,2,1)_i = Q_i(3,2,1/6) + L_i(1,2,-1/2), \quad (7)$$

$$\begin{aligned}
\bar{F}_i &= (\bar{4},1,\bar{2})_i\\
&= u_i^c(\bar{3},1,-2/3) + d_i^c(\bar{3},1,1/3)\\
&\quad + e_i^c(1,1,1) + \nu_i^c(1,1,0).
\end{aligned} \quad (8)$$

Note that the fermionic multiplet $\bar{F}_i$ additionally contains the RHNs ν_i^c; hence SM neutrinos naturally get tiny masses through a type-I seesaw mechanism [36–40]. This same seesaw scale determines the cosmic string network formation scale, and as aforementioned, the new PTA data prefer this scale to be of order $\sim 10^{15}$ GeV.

The model we explore consists of the symmetry-breaking chain given in Eq. (4), i.e.,

$$G_{422} \xrightarrow[\langle\Sigma\rangle]{M_X} G_{3221} \xrightarrow[\langle\Delta\rangle]{M'} G_{3211} \xrightarrow[\langle H\rangle+\langle\bar{H}\rangle]{M} G_{\rm SM} \xrightarrow[\langle h\rangle]{M_{\rm EW}} G_{31}. \quad (9)$$

Here, M_X refers to the Pati-Salam-breaking scale. From the discussion of the previous section, one finds that M' and M are the monopole creation scale and cosmic string formation scale, respectively. At M, since $B-L$ symmetry is broken by two units, RHNs acquire their superheavy masses. Moreover, inflation, for which we employ the standard hybrid inflation, is also associated with this latter symmetry-breaking scale. Formation of a metastable cosmic string

network showing consistency of recent PTA data requires $M' \sim M \sim 10^{15}$ GeV. As for the Pati-Salam-breaking scale, we choose $10^{16} \lesssim M_X \lesssim 10^{18}$ GeV.

The above symmetry-breaking chain proceeds through the following set of Higgs representations:

$$h = (1,2,\bar{2})_H = H_u\left(1,2,\frac{1}{2}\right) + H_d\left(1,2,-\frac{1}{2}\right), \quad (10)$$

$$\begin{aligned}\bar{H} &= (\bar{4},1,\bar{2})_H \\ &= u^c_H\left(\bar{3},1,-\frac{2}{3}\right) + d^c_H\left(\bar{3},1,\frac{1}{3}\right) \\ &\quad + e^c_H(1,1,1) + \nu^c_H(1,1,0),\end{aligned} \quad (11)$$

$$\begin{aligned}H &= (4,1,2)_H \\ &= \bar{u}^c_H\left(3,1,\frac{2}{3}\right) + \bar{d}^c_H\left(3,1,-\frac{1}{3}\right) \\ &\quad + \bar{e}^c_H(1,1,-1) + \bar{\nu}^c_H(1,1,0),\end{aligned} \quad (12)$$

$$\Delta = (1,1,3)_H = \Delta_{-1}(1,1,-1) + \Delta_0(1,1,0) + \Delta_1(1,1,1), \quad (13)$$

$$\begin{aligned}\Sigma &= (15,1,1)_H \\ &= \Sigma_0(1,1,0) + \Sigma_{2/3}(3,1,2/3) \\ &\quad + \Sigma_{-2/3}(\bar{3},1,-2/3) + \Sigma_8(8,1,0),\end{aligned} \quad (14)$$

where decomposition of these multiplets under the SM gauge group are presented.

Within the SUSY context, a flat direction to obtain inflation naturally takes place in the R-symmetric scenario. A gauge singlet superfield $S = (1,1,1)$ plays the role of the inflaton (the scalar component of it), which carries a full $U(1)_R$ charge (whereas, $H, \bar{H}, \Sigma, \Delta$ carry zero R charge). Hence, the last intermediate scale symmetry breaking as well as inflation take place via the following superpotential:

$$W_{\text{Inflation}} \supset \kappa S(H\overline{H} - M^2), \quad (15)$$

and the first two stages of symmetry breaking proceed through terms,

$$W_{\text{PS-breaking}} \supset \kappa' S'(\Sigma^2 - m^2_\Sigma) + \kappa'' S''(\Delta^2 - m^2_\Delta), \quad (16)$$

where S', S'' are also gauge singlets and carry full R charge. In principle, terms involving S, S', S'' (each carrying full R charge) all can mix and allow additional terms, which, for simplicity, are not considered in this work.

In the first breaking, the (true) Goldstones are $(3,1,2/3) + (\bar{3},1,-2/3)$; in the second breaking, Goldstones are $(1,1,1) + (1,1,-1)$; in the third breaking, the Goldstones are $(1,1,0) + (1,1,0)$. Therefore, due to R symmetry, the would-be Goldstones will be

$$(8,1,0) \subset \Sigma, \quad (17)$$

$$(\bar{3},1,1/3) + (3,1,-1/3) \subset H, \overline{H}, \quad (18)$$

$$(\bar{3},1,-2/3) + (3,1,2/3) \subset H, \overline{H}, \Sigma, \quad (19)$$

$$(1,1,-1) + (1,1,1) \subset H, \overline{H}, \Sigma, \Delta. \quad (20)$$

To give masses to a set of submultiplets, we introduce

$$D_6 = (6,1,1)_H = D_3\left(3,1,-\frac{1}{3}\right) + \overline{D}_3\left(\bar{3},1,\frac{1}{3}\right), \quad (21)$$

which carries full R charge (two units) and allow the following interactions:

$$W_{\text{mix}} \supset HHD_6 + \overline{H}\overline{H}D_6. \quad (22)$$

Because of the above interactions, they give masses to $(3,1,-1/3) + (\bar{3},1,1/3) \subset H, \overline{H}$ of order $\langle H \rangle = \langle \overline{H} \rangle \sim 10^{15}$ GeV. A similar mechanism for the rest of the would-be Goldstones cannot be implemented.

Therefore, the rest of the would-be Goldstones will acquire only SUSY-breaking masses (due to $\langle S \rangle \sim M_{\text{SUSY}}$). We also point out that extra Goldstones may result if no mixing terms are there between two multiplets carrying submultiplets with the same quantum numbers, namely, $(\overline{3},1,-2/3) + (3,1,2/3)$ and $(1,1,-1) + (1,1,1)$. The following mixing terms can be written down that can also provide SUSY scale masses to these would-be Goldstones:

$$W_{\text{mix}} \supset H\overline{H}(\Sigma + \Delta)\frac{S}{\Lambda}. \quad (23)$$

In summary, in the model under consideration, supermultiplets that reside at the SUSY scale are

$$\begin{aligned}&2 \times \{(3,1,2/3) + (\bar{3},1,-2/3)\} \\ &\quad + 2 \times \{(1,1,1) + (1,1,-1)\} + 1 \times \{(8,1,0)\}.\end{aligned} \quad (24)$$

The presence of these additional light states spoils the successful gauge coupling unification of the minimal supersymmetric Standard Model (MSSM). Since gauge couplings are not necessarily unified in the Pati-Salam setup, one still has to worry about the perturbativity of the couplings at higher scales, which we discuss below.

Since the intermediate scales M' and M are expected to be very high ($M' \sim M \sim 10^{15}$ GeV), they can be somewhat close to the M_X scale. Therefore, for the running of the

gauge couplings, it is a good approximation to consider a single step symmetry breaking at the high scale,

$$G_{422} \xrightarrow{M_X} \text{MSSM} \xrightarrow{M_{\text{SUSY}}} \text{SM}. \tag{25}$$

The well-known β coefficients [56,57] for the renormalization group equations (RGEs) are [58] $(a_1, a_2, a_3)_{\text{SM}} = (41/10, -19/6, -7)$ and $(a_1, a_2, a_3)_{\text{MSSM}} = (33/5, 1, -3)$. Moreover, for our scenario with the aforementioned additional states, we get $(a_1, a_2, a_3) = (61/5, 1, 2)_{\text{MSSM+extra}}$. We run the corresponding RGEs from the low scale to the M_X scale. By considering one-loop RGE analysis, we find that, at $M_X = 10^{16}$ GeV, the gauge couplings take the values $(g_1, g_2, g_3) = (4.08, 0.68, 1.97)$ for $M_{\text{SUSY}} = 3$ TeV and $(g_1, g_2, g_3) = (2.33, 0.67, 1.59)$ for $M_{\text{SUSY}} = 10$ TeV. On the other hand, if we set $M_X = 10^{18}$ GeV, perturbativity of the couplings requires $M_{\text{SUSY}} \geq 5000$ TeV. Therefore, in this setup, to ensure perturbativity it is safer to consider $M_{\text{SUSY}} \geq 5000$ TeV (obtained from the crude estimation mentioned above).

Before closing this section, we write down the Yukawa part of the Lagrangian, which takes the following form:

$$W_Y \supset yF\overline{F}h + \frac{y_N}{\Lambda}\overline{F}\overline{F}HH, \tag{26}$$

where Λ denotes a cutoff scale such that $\Lambda > M_X$. The last term in the above superpotential provides Majorana mass for the RHNs when the last stage of the symmetry takes place.

A unique prediction of grand unified theories is gauge-mediated proton decay. However, partial unified theories, such as gauge theories based on Pati-Salam models, are free from gauge-mediated proton decay.

V. DETAILS OF INFLATION AND BARYON ASYMMETRY

Minimal supersymmetric μ-hybrid inflation employs a canonical Kähler potential and a unique renormalizable superpotential W which respects a $U(1)R$ symmetry as [59]

$$W = \kappa S(H\overline{H} - M^2) + \lambda Sh^2, \tag{27}$$

where κ and λ are dimensionless real parameters. The scalar part of the gauge singlet chiral superfield S serves as the inflaton. The parameter M, which has mass dimensions, represents the nonzero VEV of chiral superfields H and $\overline{H}$.

The superpotential W and superfield S possess two units of R charges, while the remaining superfields are assigned zero R charges. Consequently, in the supersymmetric limit, the VEV of the scalar component of superfield S is zero. However, due to gravity-mediated supersymmetry breaking, the scalar component of S acquires a nonzero VEV proportional to $m_{3/2}$ as pointed out in [59].

The last term in the superpotential, λSh^2, effectively accounts for the μ term, where $\mu \sim (\lambda/\kappa)m_{3/2}$. This solution to the MSSM μ problem is described in [59]. The minimal canonical Kähler potential is given by

$$K_c = |S|^2 + |H|^2 + |\overline{H}|^2 + |h|^2. \tag{28}$$

Considering the effects of well-established radiative corrections [60], supergravity (SUGRA) corrections [61], and the soft supersymmetry-breaking terms [62], the inflationary potential, which arises along the D-flat direction with $|H| = |\overline{H}| = 0$ and $h = 0$, can be approximately expressed as follows:

$$V \simeq \kappa^2 M^4 \left[1 + \left(\frac{M}{m_P}\right)^4 \frac{x^4}{2} + \frac{\kappa^2}{8\pi^2}F(x) + \frac{\lambda^2}{4\pi^2}F(y) + a\left(\frac{m_{3/2}x}{\kappa M}\right) + \left(\frac{M_S x}{\kappa M}\right)^2\right], \tag{29}$$

where $x = |S|/M$, $y = \sqrt{\gamma}x$, and M_S is the soft mass of the singlet. The parameter γ is defined as $\gamma = \lambda/\kappa$, and m_P stands for the reduced Planck mass. The radiative corrections are described by the function

$$F(x) = \frac{1}{4}\left[(x^4+1)\ln\frac{(x^4-1)}{x^4} + 2x^2\ln\frac{x^2+1}{x^2-1} + 2\ln\frac{\kappa^2M^2x^2}{Q^2} - 3\right], \tag{30}$$

and the coefficient of the soft SUSY-breaking linear term is defined as

$$a = 2|A-2|\cos(\arg S + \arg|A-2|). \tag{31}$$

Both the linear term (a) and the mass-squared (M_S^2) soft SUSY-breaking terms in Eq. (29) are obtained in a gravity-mediated SUSY-breaking scheme. It Is important to note that we will focus only on the real component of S, denoted as $\sigma = |S|/\sqrt{2}$, where both the superfield and its scalar component are denoted by S.[1]

At the end of the inflation epoch, the vacuum energy is converted into the energies of coherent oscillations of the inflaton S and the scalar field $\theta = (\delta H + \delta\overline{H})/\sqrt{2}$, which subsequently decay, giving rise to radiation in the Universe. The μ-term coupling λSh^2 in Eq. (27) leads to the inflaton's decay mostly into Higgsinos, with a decay width given by [64]

$$\Gamma_1 = \frac{\lambda^2}{8\pi}m_{\text{inf}}, \tag{32}$$

[1]The imaginary component of S is neglected here, which has been studied in [63].

where $m_{\rm inf} = \sqrt{2\kappa^2 M^2 + M_S^2}$ represents the inflaton mass. The alternative decay channel for the inflaton is the decay to the right-handed neutrino through a dimension-five operator $\beta_{ij} HHN_i^c N_j^c/M^*$, which is another potential process. Heavy Majorana masses for the right-handed neutrinos are provided by the following term:

$$M_{\nu_{ij}^c} = \beta'_{ij} \frac{\langle H\rangle\langle H\rangle}{M^*}. \tag{33}$$

Also, Dirac neutrino masses on the order of the electroweak scale are obtained from the tree-level superpotential term $y_{\nu ij} N_i^c L_j H_u \to m_{\nu_D ij} N N^c$. Thus, the neutrino sector is

$$W \supset m_{\nu_D ij} N_i N_j^c + M_{\nu_{ij}^c} N_i^c N_j^c. \tag{34}$$

The small neutrino masses supported by neutrino oscillation experiments are obtained by integrating out the heavy right-handed neutrinos and read as

$$m_{\nu_{D_{\alpha\beta}}} = -\sum_i y_{\nu_{i\alpha}} y_{\nu_{i\beta}} \frac{v_u^2}{M_i}. \tag{35}$$

The neutrino mass matrix $m_{\nu_{D_{\alpha\beta}}}$ can be diagonalized by a unitary matrix $U_{\alpha i}$ as $m_{\nu_{D_{\alpha\beta}}} = U_{\alpha i} U_{\beta i} \hat{m}_{\nu_{D_i}}$, where $\hat{m}_{\nu_{D_i}}$ is a diagonal mass matrix $m_{\nu_D} = \mathrm{diag}(m_{\nu_1}, m_{\nu_2}, m_{\nu_3})$ and M_i represents the eigenvalue of mass matrix $M_{\nu_{ij}^c}$. Then the decay width for the inflaton decay into RH neutrinos is given by

$$\Gamma_2 = \frac{m_{\rm inf}}{8\pi} \left(\frac{M_N}{M}\right)^2 \left(1 - \frac{4M_N^2}{m_{\rm inf}^2}\right)^{1/2}. \tag{36}$$

The reheat temperature T_R is estimated to be [65]

$$T_R \approx \sqrt[4]{\frac{90}{\pi^2 g_*}} \sqrt{\Gamma m_P}, \qquad \Gamma = \Gamma_1 + \Gamma_2, \tag{37}$$

where g_* takes the value 228.75 for MSSM. The lepton asymmetry is generated through right-handed neutrino decays. The lepton number density to the entropy density in the limit $T_R < M_1 \equiv M_N \le m_{\rm inf}/2 \le M_{2,3}$ is defined as

$$\frac{n_L}{s} \sim \frac{3}{2} \left(\frac{\Gamma_2}{\Gamma}\right) \frac{T_R}{m_{\rm inf}} \epsilon_{cp}, \tag{38}$$

where ϵ_{cp} is the CP asymmetry factor and is generated from the out of equilibrium decay of lightest right-handed neutrino and is given by

$$\epsilon_{cp} = -\frac{3}{8\pi} \frac{1}{(y_\nu y_\nu^\dagger)_{11}} \sum_{i=2,3} \mathrm{Im}[(y_\nu y_\nu^\dagger)_{1i}]^2 \frac{M_N}{M_i}. \tag{39}$$

Assuming a normal hierarchical pattern of light neutrino masses, the CP asymmetry factor ϵ_{cp} becomes

$$\epsilon_{cp} = \frac{3}{8\pi} \frac{M_N m_{\nu_3}}{v_u^2} \delta_{\rm eff}, \tag{40}$$

where m_{ν_3} is the mass of the heaviest light neutrino, $v_u = \langle H_u\rangle$ is the VEV of the up-type electroweak Higgs interaction, and $\delta_{\rm eff}$ is the CP-violating phase. A successful baryogenesis is usually achieved through the sphaleron process where an initial lepton asymmetry n_L/s is partially converted into the baryon asymmetry as $n_B/s \sim 0.35 n_L/s$ [66]. From the experimental value of the baryon-to-photon ratio $n_B \approx (6.1 \pm 0.4) \times 10^{-10}$ [67], the required lepton asymmetry is found to be

$$|n_L/s| \approx (2.67 - 3.02) \times 10^{-10}. \tag{41}$$

In the numerical estimates discussed below, we take $m_{\nu_3} = 0.05$ eV and $v_u = 174$ GeV, while assuming large $\tan\beta$. The nonthermal production of lepton asymmetry n_L/s is given by the following expression:

$$\frac{n_L}{s} \lesssim 3 \times 10^{-10} \left(\frac{\Gamma_2}{\Gamma}\right) \left(\frac{T_R}{m_{\rm inf}}\right) \left(\frac{M_N}{10^6\,\mathrm{GeV}}\right) \left(\frac{m_{\nu_3}}{0.05\,\mathrm{eV}}\right), \tag{42}$$

with $M_1 \gg T_R$. To ensure inflationary predictions are in line with leptogenesis, we employ Eq. (42) for our numerical analysis.

VI. NUMERICAL RESULTS

The prediction for the various inflationary parameters are calculated using the standard slow-roll parameters,

$$\epsilon = \frac{1}{4}\left(\frac{m_P}{M}\right)^2 \left(\frac{V'}{V}\right)^2, \qquad \eta = \frac{1}{2}\left(\frac{m_P}{M}\right)^2 \left(\frac{V''}{V}\right),$$
$$\xi^2 = \frac{1}{4}\left(\frac{m_P}{M}\right)^4 \left(\frac{V'V'''}{V^2}\right). \tag{43}$$

In the above, the prime denotes the derivative with respect to x. Moreover, the scalar spectral index n_s, the tensor-to-scalar ratio r, and the running of the scalar spectral index $\alpha_s \equiv dn_s/d\ln k$ in the slow-roll approximation are given by

$$n_s \simeq 1 + 2\eta - 6\epsilon, \quad r \simeq 16\epsilon, \quad \alpha_s \simeq 16\epsilon\eta - 24\epsilon^2 - 2\xi^2, \tag{44}$$

with $n_s = 0.9665 \pm 0.0038$ [68] in the Λ cold dark matter model. The amplitude of the scalar power spectrum is given by

$$A_s(k_0) = \frac{1}{24\pi^2 \epsilon(x_0)} \left(\frac{V(x_0)}{m_P^4}\right), \tag{45}$$

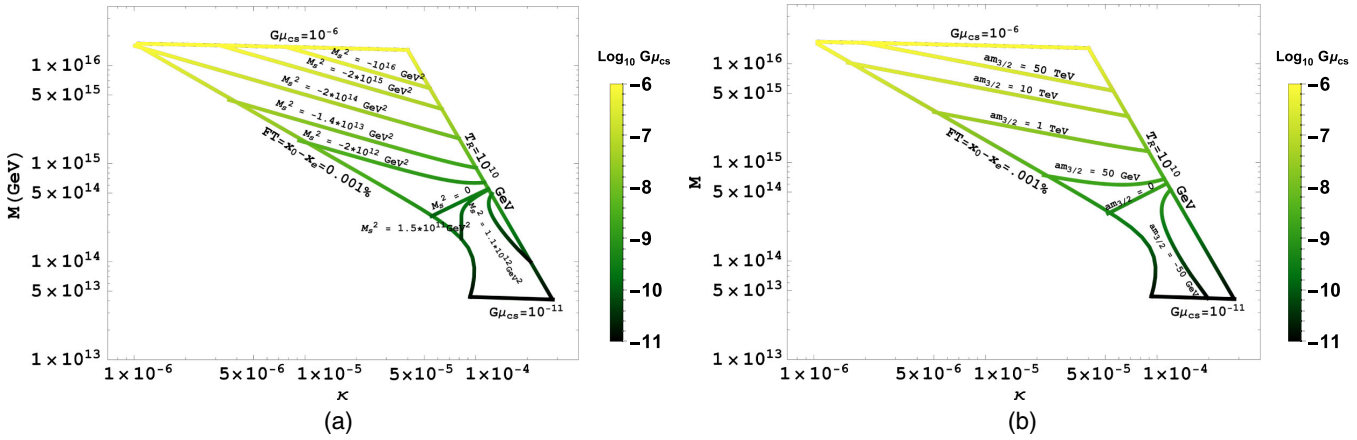

FIG. 1. The relationship between the symmetry-breaking scale (M) and the coupling strength (κ) is depicted. The reheat temperature (T_R) is bounded between a maximum of 10^{10} GeV and a minimum of 2.3×10^6 GeV and a fine-tuning bound of 0.001% is applied. An avocado colored vertical bar represents the variation of the dimensionless string tension $G\mu_{cs}$ from 10^{-6} to 10^{-11}. The inside mesh shows the variation of soft mass M_S^2 in (a) and that of $m_{3/2}$ in (b).

which at the pivot scale $k_0 = 0.05\ \mathrm{Mpc}^{-1}$ is given by $A_s(k_0) = 2.137 \times 10^{-9}$, as measured by Planck 2018 [68]. The number of e-folds N_0 is given by

$$N_0 = 2\left(\frac{M}{m_P}\right)^2 \int_{x_e}^{x_0} \left(\frac{V}{V'}\right) dx, \tag{46}$$

where $x_0 \equiv x(k_0)$ and x_e are the field values at the pivot scale k_0 and at the end of inflation, respectively. The value of x_e is determined by the breakdown of the slow-roll approximation. Finally, the number of e-folds N_0 can be written in terms of the reheat temperature [69] (assuming a standard thermal history),

$$N_0 = 53 + \frac{1}{3}\ln\left[\frac{T_R}{10^9\ \mathrm{GeV}}\right] + \frac{2}{3}\ln\left[\frac{\sqrt{\kappa}M}{10^{15}\ \mathrm{GeV}}\right]. \tag{47}$$

In our numerical analysis, we have seven independent key parameters: κ, M, $am_{3/2}$, M_S^2, x_0, x_e, and M_N. These parameters are subject to five essential constraints:

(i) the amplitude of the scalar power spectrum, denoted as $A_s(k_0)$, with a specific value of 2.137×10^{-9} [as given in Eq (45)];
(ii) the scalar spectral index, represented by n_s, which holds a fixed value of 0.9665 [68];
(iii) the end of inflation, determined by the waterfall mechanism, with the condition that $x_e = 1$;
(iv) the number of e-folds, denoted as N_0 in Eq. (46); is defined in terms of T_R by Eq. (47);
(v) the observed value of the baryon asymmetry, which translates a bound on lepton asymmetry expressed as n_L/s, which takes the specific value of 3×10^{-10} [as given in Eq. (42)].

These constraints are really important and play a crucial role for figuring out different possibilities in the model's predictions. When we take these constraints into account, we end up with two independent parameters that we can vary freely. We choose these parameters to be $am_{3/2}$ and M_S^2. By fixing one of these parameters, we can then explore the variations of the other.

We displayed our numerical calculations in Fig. 1, which illustrates how the parameters change across the $\kappa - M$ plane. During our analysis, we kept the scalar spectral index at the central value allowed by Planck, which is $n_s = 0.9655$ [68]. To make sure the SUGRA expansion does not go out of control, we required $S_0 \leq m_p$ in our parametric space. Further, we restrict $M \leq 2 \times 10^{16}$ and $T_R \leq 10^{10}$ GeV to avoid the gravitino problem [70,71]. By applying these constraints, we obtained a slice in the $\kappa - M$ plane, outlining the parameter space for inflationary predictions. We kept the plan fixed and depicted the variations of different parameters within this plane. The color-coded avocado bar illustrates how the cosmic string tension parameter varies accordingly. Note that, although the recent PTA data prefer $M \sim 10^{15}$ GeV, in presenting our results, we try to be as general as possible and vary this scale in the range $10^{13} \lesssim M \lesssim 10^{16}$ GeV. The explored parameter space yields a reheating temperature within the range of $(10^6$–$10^9)$ GeV.[2] We further restrict our numerical results by imposing the following conditions:

$$m_{\mathrm{inf}} \geq 2M_N, \qquad M_N \geq 10T_R, \tag{48}$$

which ensures successful reheating with nonthermal leptogenesis. The boundary curves in Fig. 1 represent

[2]In our model, the reheating temperature lies within the range of $(10^6$–$10^9)$ GeV. The constraints on the reheating temperature T_R and gravitino mass $m_{3/2}$ arising from the big bang can be readily met within the parameter space discussed here, for both scenarios, namely, gravitino as the stable and unstable particle. For more details, see [24].

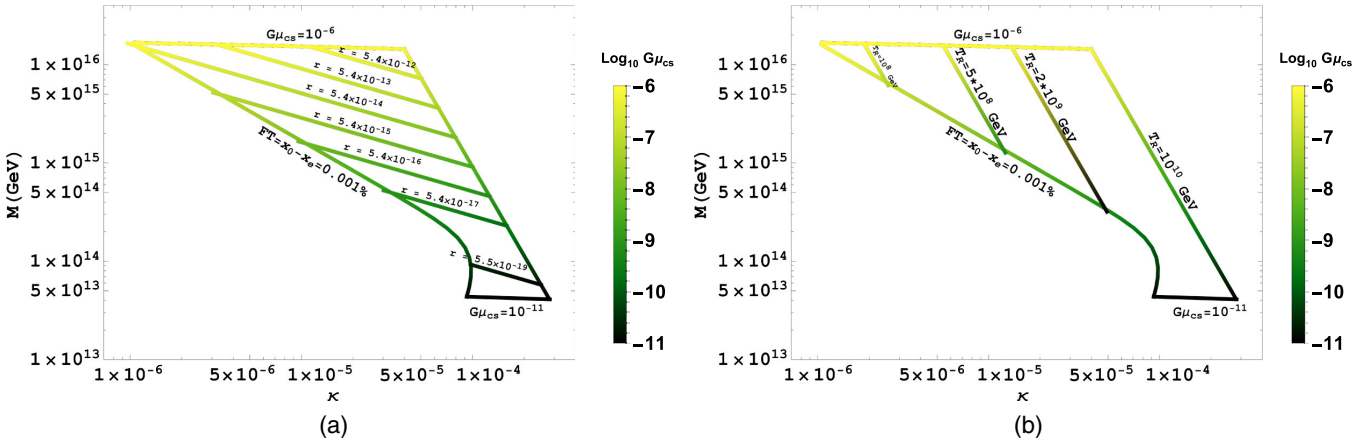

FIG. 2. The relationship between the symmetry-breaking scale (M) and the coupling strength (κ) is depicted. The reheating temperature (T_R) is bounded between a maximum of 10^{10} GeV and a minimum of 2.3×10^6 GeV and a fine-tuning bound of 0.001% is applied. An avocado colored vertical bar represents the variation of the dimensionless string tension $G\mu_{\rm cs}$ from 10^{-6} to 10^{-11}. The inside mesh shows the variation of tensor-to-scalar ratio r in (a) and the reheating temperature T_R in (b).

$M = 2 \times 10^{16}$ GeV, $T_R = 10^{10}$ GeV, $FT = 0.001\%$, and $G\mu_{\rm cs} = 10^{-11}$ constraints. In Fig. 1(a), we explore the variation of $am_{3/2}$ across a range of M_S^2 values, spanning from 2×10^{12} to -2×10^{17} GeV^2. Similarly, Fig. 1(b) demonstrates the variation of M_S^2 while keeping $m_{3/2}$ fixed within the interval of 0–730 TeV (0–155 GeV) for the cases where a is 1 or -1.

In order to achieve a red-tilted scalar spectral index consistent with Planck 2018 data, at least one of the two parameters, M_S^2 or $am_{3/2}$, is expected to be negative [72,73]. The scalar spectral index, in the limit $x_0 \sim 1$, can be approximated in the following way:

$$n_s \simeq 1 + \left(\frac{m_P}{M}\right)^2 \left(2\left(\frac{M_S}{\kappa M}\right)^2 + 3\frac{\kappa^2}{8\pi^2} F''(x_0)\right). \tag{49}$$

In the above expression, when the M_S^2 term is dominant, we obtain

$$\left(\frac{M_S}{\kappa M}\right)^2 \simeq -\frac{(1-n_s)}{2}\left(\frac{M}{m_P}\right)^2. \tag{50}$$

Hence, the consistent pattern of the curves in Fig. 1(a) across most of the upper region, displaying $M \propto \kappa^{-1/2}$ behavior, can be readily comprehended when considering constant values of M_S^2. Conversely, the $M \propto \kappa$ behavior observed near the curve where $M_S \sim 0$ can be attributed to the predominant radiative term within Eq. (49).

Regarding the behavior of the corresponding curves in Fig. 1(b) with constant values of $am_{3/2} > 0$, a competition arises among the soft SUSY-breaking terms in $\epsilon(x_0)$ to meet the constraint imposed by A_s in Eq. (45). This observation, combined with Eq. (49), leads to the emergence of a $M \propto \kappa^{-1/3}$ behavior. This behavior aligns with the curves exhibited in the upper region of Fig. 1(b).

In scenarios where $M_S^2 > 0$, as we depart from the $M_S \sim 0$ curve in Fig. 1(a), the radiative corrections compete with the M_S^2 term in Eq. (49). Consequently, we discern that the parameter M varies in proportion to κ^{-2}, as clearly observed in the lower region of Fig. 1(a).

Now, focusing on the corresponding region displayed in Fig. 1(b) and holding constant values of $am_{3/2} > 0$, in order to satisfy the constraint on the amplitude of the scalar power spectrum A_s as delineated in Eq. (45), the contributions from both soft SUSY breaking and radiative corrections become comparable within the expression for $\epsilon(x_0)$. This behavior is characterized by $M \propto \kappa^{-3}$ for the curves featured in the lower part of Fig. 1(b).

In Fig. 2, in the $\kappa - M$ plane, the left panel depicts the variation of the tensor-to-scalar ratio r, while the right panel illustrates the variation of the reheating temperature T_R. The predicted range of the tensor-to-scalar ratio is tiny and lies in the range $r \sim 5 \times 10^{-11}$–5×10^{-21}, see Fig. 2(a). The various curves with constant values of r show $M \propto \kappa^{-1/2}$ behavior, as can be deduced from Eq. (45),

$$r \sim \frac{2}{3\pi^2 A_s(k_0)} \frac{\kappa^2 M^4}{m_P^4}. \tag{51}$$

Similarly, in Fig. 2(b), the curves with fixed values of reheat temperature in the range of $T_R \in [2 \times 10^6$–$10^{10}]$ GeV follow $M \propto \kappa^{-3}$ behavior obtained from Eq. (37). For the scalar spectral index n_s fixed at Planck's central value (0.9655), we obtain the following ranges of remaining parameters:

$$1.3 \times 10^{-7} \lesssim \kappa \lesssim 2.1 \times 10^{-4},$$
$$(1.3 \times 10^{13} \lesssim M \lesssim 2.0 \times 10^{16})\ \text{GeV},$$
$$10^{-11} \lesssim G\mu_{CS} \lesssim 8 \times 10^{-6}.$$

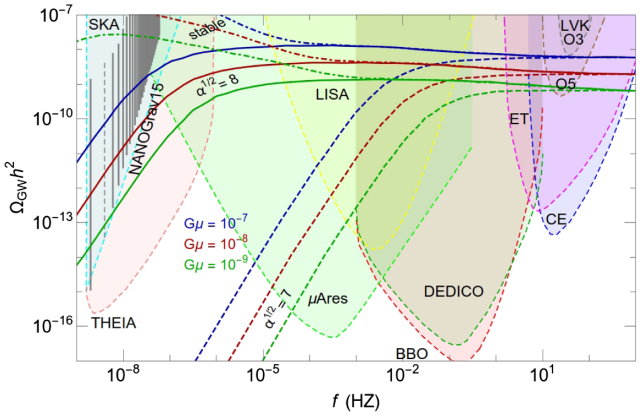

FIG. 3. Gravitational wave signal from metastable cosmic strings explaining the recent PTA result [6] [in particular, the one with $(G\mu, \alpha^{1/2}) = (10^{-7}, 8)$, see text for details]. For metastable cosmic string networks, we demonstrate the GW signals for two different values of the decay parameters, namely, $\alpha^{1/2} = 8$ (solid lines) and $\alpha^{1/2} = 7$ (dashed lines). Moreover, the GW spectrum is presented for three different values of the string tension: $G\mu = 10^{-7}$ (blue), $G\mu = 10^{-8}$ (red), and $G\mu = 10^{-9}$ (green). For comparison, the GW spectrum from a stable cosmic string network is depicted with dash-dotted lines. The current LVK [75,76] bound (O3) on cosmic string networks is depicted. Future sensitivities of various upcoming experiments, such as LISA [77], SKA [78], THEIA [79] (see also [80,81]), ET [82], CE [83], BBO [84], and DECIGO [85], are also illustrated.

All the solutions obtained in our analysis satisfy the leptogenesis constraint, as depicted in Eq. (42).

Furthermore, as mentioned before, the gauge-breaking scale, denoted by M, is related to the cosmic string tension parameters μ_{cs}. The vertical avocado bar in the plot indicates the range of the string tension parameter $G\mu_{\rm cs}$, which for making the plots, is varied in the range $\sim 10^{-6}$–10^{-11}. However the cosmic microwave background (CMB) constraint $G\mu_{\rm cs} \leq 1.3 \times 10^{-7}$ on cosmic string tension limits M to be less than or equal to 1.8×10^{15}. Within this M range, κ falls in the range of 8.9×10^{-6}–2.1×10^{-4} as depicted in Figs. 1 and 2. This favored parameter space aligns with stochastic gravitational wave backgrounds, contingent on the selection of M and adjustment of $\sqrt{\alpha}$. As pointed out in Sec. II, the third advanced LVK bound rules out regions of the parameter space for $G\mu_{\rm cs} > 10^{-7}$ [6], whereas the recent PTA data strongly suggest $G\mu_{\rm cs} \sim 10^{-7}$ for $\sqrt{\alpha}$ close to 8 [6]. This LVK bound is slightly stronger than the constraints arising from CMB, which leads to $G\mu_{\rm cs} \lesssim 1.3 \times 10^{-7}$ [68,74]. Intriguingly, the entire region of the parameter space shown in all these plots above, with $G\mu_{\rm cs} < 10^{-7}$ in a broad spectrum of frequencies, will be fully probed by several gravitational wave observatories. This is explicitly depicted in Fig. 3 for an example parameter point with $(G\mu_{\rm cs}, \alpha^{1/2}) = (10^{-7}, 8)$, which explains the recent PTA data. In Fig. 3, the GW spectrum is shown for three different values of the string tension: $G\mu = 10^{-7}$ (blue), $G\mu = 10^{-8}$ (red), and $G\mu = 10^{-9}$ (green). Moreover, for metastable cosmic string networks, we demonstrate the GW signals for two different values of the decay parameters, namely, $\alpha^{1/2} = 8$ (solid lines) and $\alpha^{1/2} = 7$ (dashed lines). The GW spectrum from a stable cosmic string network is illustrated with dash-dotted lines for comparison. For making this plot, we followed the procedure explained in Ref. [20].

Note that, using the PTAs, it may also be possible to detect stochastic GW background to the ultralow frequency, in particular, for $f \sim 10^{-12}$–10^{-9} Hz [86]. The analysis performed in [86] using the current PTA data shows sensitivity for $\Omega_{\rm GW}h^2 \gtrsim 10^{-8}$, which is not of our interest.

VII. CONCLUSIONS

In conclusion, we have investigated promising pathways for model building that connect the Pati-Salam model to the Standard Model, uncovering noteworthy cosmological implications along the way. The breaking pattern G_{422} to G_{3211} through G_{3221} produces monopoles. To circumvent the issue of monopoles, we adopted the standard SUSY hybrid inflation at G_{3211} scale, ensuring compatibility with matter-antimatter asymmetry obtained through leptogenesis. Our model not only produces a scalar tilt that aligns with the Planck 2018 constraints but also exhibits small tensor modes beyond the scope of upcoming CMB experiments. The breaking of G_{3211} at the end of inflation leads to the cosmic strings, which eventually disappear due to the quantum tunneling of the monopole-antimonopole pairs, confirming the formation of a metastable cosmic string network. The stochastic gravitational wave background produced by this network of metastable strings is compatible with the gravitational waves observed recently by pulsar timing array experiments, including NANOGrav, CPTA, EPTA, InPTA, and PPTA. Furthermore, this gravitational wave spectrum remains within the detection capabilities of both existing and future ground- and space-based experiments.

ACKNOWLEDGMENTS

T. A. C. would like to thank the High Energy Theory Group in the Department of Physics and Astronomy at the University of Kansas for their hospitality and support. The work of S. N. is supported by the United Arab Emirates University (UAEU) under UAEU Program for Advanced Research (UPAR) Grant No. 12S093. S. S. would like to thank Qaisar Shafi for discussion and Kevin Hinze for his help in preparing Fig. 3.

[1] NANOGrav Collaboration, The NANOGrav 15 yr data set: Evidence for a gravitational-wave background, Astrophys. J. Lett. **951**, L8 (2023).

[2] EPTA Collaboration, The second data release from the European Pulsar Timing Array III. Search for gravitational wave signals, Astron. Astrophys. **678**, A50 (2023).

[3] D. J. Reardon *et al.*, Search for an isotropic gravitational-wave background with the Parkes Pulsar Timing Array, Astrophys. J. Lett. **951**, L6 (2023).

[4] H. Xu *et al.*, Searching for the nano-hertz stochastic gravitational wave background with the Chinese Pulsar Timing Array Data Release I, Res. Astron. Astrophys. **23**, 075024 (2023).

[5] NANOGrav Collaboration, The NANOGrav 15 yr data set: Constraints on supermassive black hole binaries from the gravitational-wave background, Astrophys. J. Lett. **952**, L37 (2023).

[6] NANOGrav Collaboration, The NANOGrav 15 yr data set: Search for signals from new physics, Astrophys. J. Lett. **951**, L11 (2023).

[7] EPTA Collaboration, The second data release from the European Pulsar Timing Array: V. Implications for massive black holes, dark matter and the early Universe, arXiv:2306.16227.

[8] S. Antusch, K. Hinze, S. Saad, and J. Steiner, Singling out SO(10) GUT models using recent PTA results, Phys. Rev. D **108**, 095053 (2023).

[9] W. Buchmuller, V. Domcke, and K. Schmitz, Metastable cosmic strings, J. Cosmol. Astropart. Phys. 11 (2023) 020.

[10] B. Fu, S. F. King, L. Marsili, S. Pascoli, J. Turner, and Y.-L. Zhou, Testing realistic $SO(10)$ SUSY GUTs with proton decay and gravitational waves, arXiv:2308.05799.

[11] G. Lazarides, R. Maji, A. Moursy, and Q. Shafi, Inflation, superheavy metastable strings and gravitational waves in non-supersymmetric flipped SU(5), arXiv:2308.07094.

[12] W. Ahmed, M. U. Rehman, and U. Zubair, Probing stochastic gravitational wave background from $SU(5) \times U(1)_\chi$ strings in light of NANOGrav 15-year data, arXiv:2308.09125.

[13] R. Maji and W.-I. Park, Supersymmetric $U(1)_{B-L}$ flat direction and NANOGrav 15 year data, arXiv:2308.11439.

[14] A. Afzal, M. Mehmood, M. U. Rehman, and Q. Shafi, Supersymmetric hybrid inflation and metastable cosmic strings in $SU(4)_c \times SU(2)_L \times U(1)_R$, arXiv:2308.11410.

[15] W. Buchmuller, V. Domcke, H. Murayama, and K. Schmitz, Probing the scale of grand unification with gravitational waves, Phys. Lett. B **809**, 135764 (2020).

[16] J. A. Dror, T. Hiramatsu, K. Kohri, H. Murayama, and G. White, Testing the seesaw mechanism and leptogenesis with gravitational waves, Phys. Rev. Lett. **124**, 041804 (2020).

[17] S. F. King, S. Pascoli, J. Turner, and Y.-L. Zhou, Gravitational waves and proton decay: Complementary windows into grand unified theories, Phys. Rev. Lett. **126**, 021802 (2021).

[18] W. Buchmuller, V. Domcke, and K. Schmitz, From NANOGrav to LIGO with metastable cosmic strings, Phys. Lett. B **811**, 135914 (2020).

[19] W. Buchmuller, Metastable strings and dumbbells in supersymmetric hybrid inflation, J. High Energy Phys. 04 (2021) 168.

[20] W. Buchmuller, V. Domcke, and K. Schmitz, Stochastic gravitational-wave background from metastable cosmic strings, J. Cosmol. Astropart. Phys. 12 (2021) 006.

[21] D. I. Dunsky, A. Ghoshal, H. Murayama, Y. Sakakihara, and G. White, GUTs, hybrid topological defects, and gravitational waves, Phys. Rev. D **106**, 075030 (2022).

[22] M. A. Masoud, M. U. Rehman, and Q. Shafi, Sneutrino tribrid inflation, metastable cosmic strings and gravitational waves, J. Cosmol. Astropart. Phys. 11 (2021) 022.

[23] W. Ahmed, M. Junaid, S. Nasri, and U. Zubair, Constraining the cosmic strings gravitational wave spectra in no-scale inflation with viable gravitino dark matter and nonthermal leptogenesis, Phys. Rev. D **105**, 115008 (2022).

[24] A. Afzal, W. Ahmed, M. U. Rehman, and Q. Shafi, μ-hybrid inflation, gravitino dark matter, and stochastic gravitational wave background from cosmic strings, Phys. Rev. D **105**, 103539 (2022).

[25] S. F. King, S. Pascoli, J. Turner, and Y.-L. Zhou, Confronting SO(10) GUTs with proton decay and gravitational waves, J. High Energy Phys. 10 (2021) 225.

[26] G. Lazarides, R. Maji, and Q. Shafi, Gravitational waves from quasi-stable strings, J. Cosmol. Astropart. Phys. 08 (2022) 042.

[27] B. Fu, S. F. King, L. Marsili, S. Pascoli, J. Turner, and Y.-L. Zhou, A predictive and testable unified theory of fermion masses, mixing and leptogenesis, J. High Energy Phys. 11 (2022) 072.

[28] S. Saad, Probing minimal grand unification through gravitational waves, proton decay, and fermion masses, J. High Energy Phys. 04 (2023) 058.

[29] R. Maji, W.-I. Park, and Q. Shafi, Gravitational waves from walls bounded by strings in $SO(10)$ model of pseudo-Goldstone dark matter, Phys. Lett. B **845**, 138127 (2023).

[30] T. W. B. Kibble, Topology of cosmic domains and strings, J. Phys. A **9**, 1387 (1976).

[31] J. C. Pati and A. Salam, Is baryon number conserved?, Phys. Rev. Lett. **31**, 661 (1973).

[32] J. C. Pati and A. Salam, Lepton number as the fourth color, Phys. Rev. D **10**, 275 (1974).

[33] R. N. Mohapatra and J. C. Pati, Left-right gauge symmetry and an isoconjugate model of CP violation, Phys. Rev. D **11**, 566 (1975).

[34] R. N. Mohapatra and J. C. Pati, A natural left-right symmetry, Phys. Rev. D **11**, 2558 (1975).

[35] G. Senjanovic and R. N. Mohapatra, Exact left-right symmetry and spontaneous violation of parity, Phys. Rev. D **12**, 1502 (1975).

[36] P. Minkowski, $\mu \to e\gamma$ at a rate of one out of 10^9 muon decays?, Phys. Lett. **67B**, 421 (1977).

[37] M. Gell-Mann, P. Ramond, and R. Slansky, Complex spinors and unified theories, Conf. Proc. C **790927**, 315 (1979).

[38] S. L. Glashow, The future of elementary particle physics, NATO Sci. Ser. B **61**, 687 (1980).

[39] R. N. Mohapatra and G. Senjanovic, Neutrino mass and spontaneous parity nonconservation, Phys. Rev. Lett. **44**, 912 (1980).

[40] T. Yanagida, Horizontal gauge symmetry and masses of neutrinos, Conf. Proc. C **7902131**, 95 (1979).

[41] M. Fukugita and T. Yanagida, Baryogenesis without grand unification, Phys. Lett. B **174**, 45 (1986).

[42] R. N. Mohapatra and R. E. Marshak, Local B-L symmetry of electroweak interactions, Majorana neutrinos and neutron oscillations, Phys. Rev. Lett. **44**, 1316 (1980).

[43] I. Antoniadis and G. K. Leontaris, A supersymmetric SU(4) × O(4) model, Phys. Lett. B **216**, 333 (1989).

[44] S. F. King and Q. Shafi, Minimal supersymmetric $SU(4) \times SU(2)_L \times SU(2)_R$, Phys. Lett. B **422**, 135 (1998).

[45] R. Jeannerot, S. Khalil, G. Lazarides, and Q. Shafi, Inflation and monopoles in supersymmetric $SU(4)_C \times SU(2)_L \times SU(2)_R$, J. High Energy Phys. 10 (2000) 012.

[46] A. Melfo and G. Senjanovic, Minimal supersymmetric Pati-Salam theory: Determination of physical scales, Phys. Rev. D **68**, 035013 (2003).

[47] T. Vachaspati and A. Vilenkin, Gravitational radiation from cosmic strings, Phys. Rev. D **31**, 3052 (1985).

[48] C. T. Hill, H. M. Hodges, and M. S. Turner, Bosonic superconducting cosmic strings, Phys. Rev. D **37**, 263 (1988).

[49] G. 't Hooft, Magnetic monopoles in unified gauge theories, Nucl. Phys. **B79**, 276 (1974).

[50] A. M. Polyakov, Particle spectrum in quantum field theory, JETP Lett. **20**, 194 (1974).

[51] P. Langacker and S.-Y. Pi, Magnetic monopoles in grand unified theories, Phys. Rev. Lett. **45**, 1 (1980).

[52] G. Lazarides, Q. Shafi, and T. F. Walsh, Cosmic strings and domains in unified theories, Nucl. Phys. **B195**, 157 (1982).

[53] A. Vilenkin, Cosmological evolution of monopoles connected by strings, Nucl. Phys. **B196**, 240 (1982).

[54] G. Lazarides and Q. Shafi, Monopoles, strings, and necklaces in $SO(10)$ and E_6, J. High Energy Phys. 10 (2019) 193.

[55] G. Lazarides, M. U. Rehman, Q. Shafi, and F. K. Vardag, Shifted μ-hybrid inflation, gravitino dark matter, and observable gravity waves, Phys. Rev. D **103**, 035033 (2021).

[56] D. R. T. Jones, The two loop β function for a $G(1) \times G(2)$ gauge theory, Phys. Rev. D **25**, 581 (1982).

[57] M. E. Machacek and M. T. Vaughn, Two loop renormalization group equations in a general quantum field theory. 1. Wave function renormalization, Nucl. Phys. **B222**, 83 (1983).

[58] H. Arason, D. J. Castano, B. Keszthelyi, S. Mikaelian, E. J. Piard, P. Ramond *et al.*, Renormalization group study of the standard model and its extensions. 1. The standard model, Phys. Rev. D **46**, 3945 (1992).

[59] G. R. Dvali, G. Lazarides, and Q. Shafi, μ Problem and hybrid inflation in supersymmetric $SU(2)_L \times SU(2)_R \times U(1)_{B-L}$, Phys. Lett. B **424**, 259 (1998).

[60] S. R. Coleman and E. J. Weinberg, Radiative corrections as the origin of spontaneous symmetry breaking, Phys. Rev. D **7**, 1888 (1973).

[61] A. D. Linde and A. Riotto, Hybrid inflation in supergravity, Phys. Rev. D **56**, R1841 (1997).

[62] M. U. Rehman, Q. Shafi, and J. R. Wickman, Supersymmetric hybrid inflation redux, Phys. Lett. B **683**, 191 (2010).

[63] W. Buchmüller, V. Domcke, K. Kamada, and K. Schmitz, Hybrid inflation in the complex plane, J. Cosmol. Astropart. Phys. 07 (2014) 054.

[64] G. Lazarides and N. D. Vlachos, Atmospheric neutrino anomaly and supersymmetric inflation, Phys. Lett. B **441**, 46 (1998).

[65] E. W. Kolb and M. S. Turner, *The Early Universe* (CRC Press, Boca Raton, 1990), Vol. 69.

[66] J. A. Harvey and M. S. Turner, Cosmological baryon and lepton number in the presence of electroweak fermion number violation, Phys. Rev. D **42**, 3344 (1990).

[67] Particle Data Group Collaboration, Review of particle physics, Prog. Theor. Exp. Phys. **2020**, 083C01 (2020).

[68] Planck Collaboration, Planck 2018 results. X. Constraints on inflation, Astron. Astrophys. **641**, A10 (2020).

[69] A. R. Liddle and S. M. Leach, How long before the end of inflation were observable perturbations produced?, Phys. Rev. D **68**, 103503 (2003).

[70] J. R. Ellis, J. E. Kim, and D. V. Nanopoulos, Cosmological gravitino regeneration and decay, Phys. Lett. **145B**, 181 (1984).

[71] M. Y. Khlopov and A. D. Linde, Is it easy to save the gravitino?, Phys. Lett. **138B**, 265 (1984).

[72] W. Ahmed, A. Karozas, G. K. Leontaris, and U. Zubair, Smooth hybrid inflation with low reheat temperature and observable gravity waves in $SU(5) \times U(1)_\chi$ super-GUT, J. Cosmol. Astropart. Phys. 06 (2022) 027.

[73] W. Ahmed and U. Zubair, Radiative symmetry breaking, cosmic strings and observable gravity waves in $U(1)_R$ symmetric $SU(5) \times U(1)_\chi$, J. Cosmol. Astropart. Phys. 01 (2023) 019.

[74] Planck Collaboration, Planck 2018 results. VI. Cosmological parameters, Astron. Astrophys. **641**, A6 (2020).

[75] LIGO Scientific, Virgo, and KAGRA Collaborations, Constraints on cosmic strings using data from the third Advanced LIGO–Virgo observing run, Phys. Rev. Lett. **126**, 241102 (2021).

[76] KAGRA, Virgo, and LIGO Scientific Collaborations, Upper limits on the isotropic gravitational-wave background from Advanced LIGO and Advanced Virgo's third observing run, Phys. Rev. D **104**, 022004 (2021).

[77] LISA Collaboration, Laser Interferometer Space Antenna, arXiv:1702.00786.

[78] G. Janssen *et al.*, Gravitational wave astronomy with the SKA Proc. Sci., AASKA14 (**2015**) 037.

[79] Theia Collaboration, Theia: Faint objects in motion or the new astrometry frontier, arXiv:1707.01348.

[80] J. Garcia-Bellido, H. Murayama, and G. White, Exploring the early Universe with Gaia and Theia, J. Cosmol. Astropart. Phys. 12 (2021) 023.

[81] F. Malbet *et al.*, Theia: Science cases and mission profiles for high precision astrometry in the future, in SPIE Astronomical Telescopes+Instrumentation 2022 (2022), 7, arXiv:2207.12540.

[82] B. Sathyaprakash *et al.*, Scientific objectives of Einstein telescope, Classical Quantum Gravity **29**, 124013 (2012).

[83] LIGO Scientific Collaboration, Exploring the sensitivity of next generation gravitational wave detectors, Classical Quantum Gravity **34**, 044001 (2017).

[84] V. Corbin and N. J. Cornish, Detecting the cosmic gravitational wave background with the big bang observer, Classical Quantum Gravity **23**, 2435 (2006).

[85] N. Seto, S. Kawamura, and T. Nakamura, Possibility of direct measurement of the acceleration of the Universe using 0.1-Hz band laser interferometer gravitational wave antenna in space, Phys. Rev. Lett. **87**, 221103 (2001).

[86] W. DeRocco and J. A. Dror, Searching for stochastic gravitational waves below a nanohertz, Phys. Rev. D **108**, 103011 (2023).